PHASE EQUILIBRIA IN THE Ag_2Te–ZnTe AND Ag_2Te–Zn SYSTEMS

V. Vassilev[1][*], *V. Parvanova*[1] *and V. Vatchkov*[2]

[1]University of Chemical Technology and Metallurgy, 8 'K. Okhridski' blvd., 1756 Sofia, Bulgaria
[2]Southwestern University 'N. Rilski', 2700 Blagoevgrad, Bulgaria

The state diagrams (T–x) of the systems Ag_2Te–ZnTe(I) and Ag_2Te–Zn(II) are offered on the ground of data obtained by differential thermal analysis, X-ray phase analysis, microstructural analysis and measurements of the density and the microhardness of samples synthesized. The systems studied are quasibinary sections of the ternary system Ag–Zn–Te.

System I is characterized by two eutectic and three eutectoidal non-variant equilibria as well as by an intermediate compound Ag_2ZnTe_2, which melts congruently at 880°C. The latter exists in the range from 120 to 880°C in two polymorphic modifications ($T_{\alpha\rightarrow\beta}$=515°C). System II is characterized by one eutectic, two eutectoidal and one peritectic nonvariant equilibria, boundary solid solutions on the ground of Ag_2Te and Zn and one intermediate phase of the composition $Ag_4Zn_3Te_2$, which melts congruently at 880°C.

*Keywords: non-variant equilibria, phase equilibria, state diagrams*

Introduction

The semiconducting compounds Ag_2Te and ZnTe are relatively new materials, whose physical, physicochemical and optical properties vary in wide ranges. The systems containing Ag_2Te and ZnTe (system I) and Ag_2Te and Zn (system II) are of research interest, because on one hand, the initial compounds have contrasting properties (Ag_2Te and ZnTe are a small band gap and a large band gap semiconductors, respectively, Zn is a metal), while on the other, the phase equilibria attained are either not studied at all (system II), or not exhaustively studied like in the case of system I.

The state diagrams of systems I and II coincide with polythermic sections of that of the three-component system Ag–Zn–Te. The outlining of a relation between the composition and the different properties in the scheme: composition $\Leftrightarrow$ structure $\Leftrightarrow$ properties is a complex problem. It requires: (*i*) a study on the phase equilibria in the three-component system along different polythermic sections to provide information on the ranges of solid solutions or the presence of new intermediate phases; (*ii*) an investigation of the properties of the materials pointed above aiming to determine the areas of their application.

The polythermic sections Ag–Zn [1, 2], Ag–Te [3, 4] and Zn–Te [5–7] of the three-component system Ag–Zn–Te have been studied. Only one compound, ZnTe, is found in Zn–Te system. It melts congruently at 1290°C and forms degenerated eutectic mixtures with its constituent substances. Several intermediate compounds are formed as well: Ag_2Te (it freezes out of a melt at 959°C); $Ag_{1.88}Te$, Ag_5Te_3 and

AgTe (they are obtained in the course of peritectic reactions at 465, 460 and 210°C, correspondingly). In the range from the ambient temperature to the melting point, Ag_2Te takes part in two polymorphic transitions. The space lattice of α-Ag_2Te is monoclinic, that of β-Ag_2Te is face-centered, while the space lattice of γ-Ag_2Te is body-centered. The deviation from the stoichiometric composition leads to a change in the temperature of the phase transitions:

$$\alpha\text{-}Ag_2Te \xrightarrow{\;105–145°C\;} \beta\text{-}Ag_2Te$$
$$\xrightarrow{\;690–802°C\;} \gamma\text{-}Ag_2Te$$
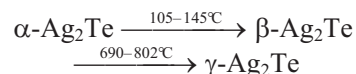
This evidences the presence of a range of homogeneity based on Ag_2Te.

The thermic width of ZnTe forbidden band at 25°C is 2.12 eV [8], while the optic width is 2.26 eV [9]. The mobility of electrons and holes at 25°C is 340 and 110 cm^2 V^{-1} s^{-1} [9], correspondingly. ZnTe has photoluminescent and electroluminescent properties. It is used for the development of solar energy systems, generators of electromagnetic radiation in the visible region of the electromagnetic spectrum, while in combination with HgTe it is used for infrared sensors [10]. α-Ag_2Te is a small gap semiconductor, whose forbidden band's width is dependent on defects concentration and is in the range from 0.064 to 0.149 eV [11–13]. The concentration and the mobility of the electrons at 25°C are 10^{18} cm^{-3} and 5000 cm^2 V^{-1} s^{-1} [14], correspondingly. Thermoelectric transformers, optical quantum generators, photoelectric receivers in the infrared region of the spectrum, etc. are constructed on the ground of α-Ag_2Te.

---

* Author for correspondence: venciv@uctm.edu

Some preliminary investigations were carried out to determine the type of the sections Ag$_2$Te–ZnTe (I) and Ag$_2$Te–Zn (II). Alloys corresponding to points A and B (Fig. 1) were synthesized using Ag$_2$Te+ZnTe (alloy A1), Ag$_2$Te+Zn (alloy B1), Te+Ag$_{2/3}$Zn$_{1/3}$ (alloy A2) and Ag+ZnTe (alloy B2), respectively. The analysis of the X-ray diffraction patterns of alloys A1, A2, B1 and B2 shows that they are two-phase systems. The lines of Ag$_2$Te and ZnTe are recorded in case of alloys A1 and A2, while those of Ag$_2$Te and Zn – in case of alloys B1 and B2. These results indicate that the polythermic sections of the three-component system Ag–Zn–Te, i.e. Ag$_2$Te–ZnTe and Ag$_2$Te–Zn, are quasi-binary, while the sections Te–Ag$_{2/3}$Zn$_{1/3}$ and Ag–ZnTe are not.

It should be noted that the phase diagram of Ag$_2$Te–ZnTe was offered by Trischuk *et al.* [15] using data from differential thermal analysis (DTA) and microstructural analysis (MSA). For compositions rich in Ag$_2$Te at $T \leq 150°$C, the boundaries of the phase regions are not determined very precisely. No intermediate compound was reported [15] for the system Ag$_2$Te–ZnTe, while our experimental results verify the presence of Ag$_2$ZnTe$_2$ [16].

The aim of the present paper is to study additionally and define more precisely the state diagram of Ag$_2$Te–ZnTe(I) using DTA [17], MSA, X-ray phase analysis (XRA) and data from measurements of the microhardness (HV) and the density (d) of the samples as well as to offer the state diagram of Ag$_2$Te–Zn(II).

Experimental

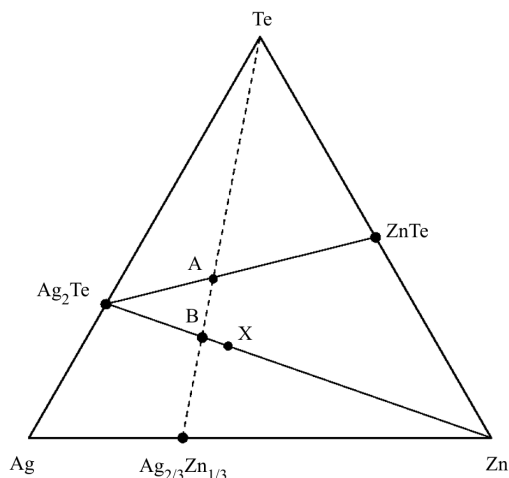The systems Ag$_2$Te–ZnTe(I) and Ag$_2$Te–Zn(II) were studied using 18 and 17 compositions within the concentration range from 0 to 100 mol% of Ag$_2$Te, cor-respondingly. The compositions were prepared through a direct mono-temperature synthesis [10] in evacuated and sealed quartz ampoules. The maximum temperature and the duration of the synthesis were 1150°C and 2 h. A vibrational stirring of the melt was applied. As a final step the melts were homogenized at 600°C for 3 h.

The phase transformation in the samples was investigated by means of several methods as follows: DTA (using equipment of the type Paulik- Paulik-Erdey made by MOM, Hungary) at the heating rate of 10°C min^{-1}, reference substance (calcinated γ-Al$_2$O$_3$) and the studied substance 0.5 g and was placed in evacuated and sealed quartz ampoules at pressure equal to 0.1 Pa; XRD (equipment TUR-M61) with CuK$_\alpha$-radiation and Ni-filter, θ=5–40°; microstructure analysis (microscope MIM-7); measurements of the microhardness (instrument PMT-3 at loading of 10 and 20 g) and of the density of the material (hydrostatic technique with toluene as reference liquid).

Results and discussion

The results from XRA of both systems' samples are presented as line-diagrams (Figs 2 and 3), which are characterized by the following peculiarities:

- the reflections of the Ag$_2$Te (system I) are shifted in direction of Bragg angle decrease (increase of plane spacing) for samples containing from 100 to 91 mol% of Ag$_2$Te (Fig. 2). The same tendency is observed when Ag$_2$Te is added to ZnTe (from 95 to 100 mol% of ZnTe). In the concentration range from 9 to 95 mol% of ZnTe, the diffraction reflections of both Ag$_2$Te and ZnTe are observed;
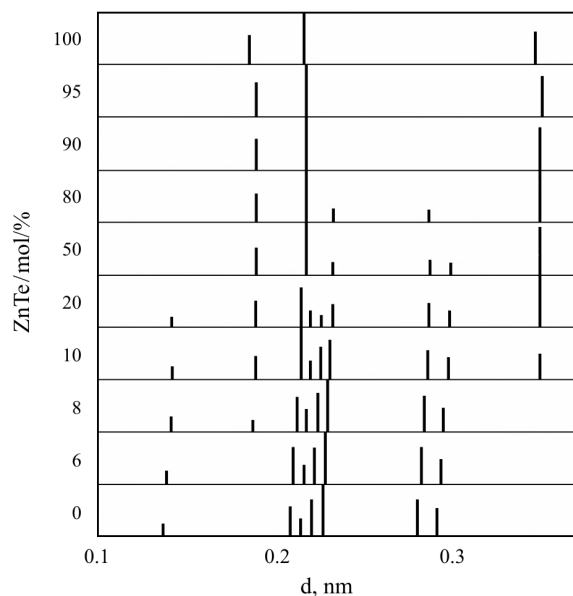

Fig. 1 Gibbs phase diagram of the ternary system Ag–Zn–Te

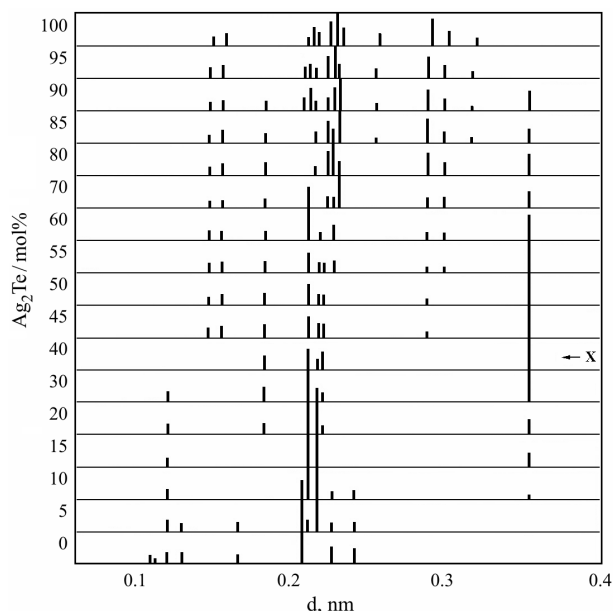**Fig. 2** Line-diagrams of samples of the system Ag$_2$Te–ZnTe

Fig. 3 Line-diagrams of samples of the system Ag$_2$Te–Zn

- new lines are observed when the composition is (Ag$_2$Te)$_{40}$Zn$_{60}$ (system II); this indicates the formation of an intermediate phase 'X' – Fig. 1;
- the diffraction lines of Ag$_2$Te are shifted in direction of plane spacing (d) decrease in the concentration range 0≤x≤5, i.e. limited solid solutions based on α-Ag$_2$Te exist in this range. The lines of two phases, α-Ag$_2$Te+X and X+Zn are observed simul-

taneously in the ranges 5≤x≤60 and 60≤x≤100. The intensity of X lines decreases on increase of Ag$_2$Te or Zn content.

The temperature value of the phase transitions in systems I and II were determined with the application of DTA. They are summarized in Tables 1 and 2.

The effects observed are endothermic and differ in area. Particularly well outlined are the effects of melting and those of the phase transition α-Ag$_2$Te ⇔ β-Ag$_2$Te at compositions richer in Ag$_2$Te. The effects of β-Ag$_2$Te ⇔ γ-Ag$_2$Te transition, those of the bimodal curve of system II and solvus-lines as well as the effects connected with the formation of the intermediate phase Ag$_2$ZnTe$_2$ (system I) are poorly outlined. Up to five endothermic effects were recorded in one and the same curve in case of some of the samples.

Two etching solutions were used to disclose the microstructure of system I samples. These were: HF:HNO$_3$:H$_2$O:CH$_3$COOH=10:10:5:1 (τ=20–30 s, T=20°C for compositions rich in Ag$_2$Te) and HF:H$_2$O$_2$:H$_2$O=2:2:3 (τ=30 s, T=30°C for compositions rich in ZnTe). The microstructure of system II samples rich in Zn was revealed during the 'polishing' step using Cr$_2$O$_3$. The etching solution HNO$_3$:CH$_3$COOH:H$_2$O=3:2:1 (τ=5–10 s, T=40°C) was used for compositions rich in Ag$_2$Te. Samples containing from 0 to 9 and from 95 to 100 mol% of ZnTe (system I) and from 0 to 5 mol% of Zn as well as

Table 1 Thermal effects observed on heating samples of the system Ag$_2$Te–ZnTe

Composition/ mol% of ZnTe	Endothermic effects on heating, T/°C								
	1	2	3	4	5	6	7	8	9
0	–	–	150	–	–	795	–	–	960
5	–	140	145	–	–	730	–	900	–
10	–	135	140	–	–	685	710	855	870
15	120	135	–	–	–	660	675	825	850
20	120	135	–	515	650	–	700	815	840
25	120	130	810	520	650	–	–	–	840
30	115	135	810	520	650	–	–	–	835
40	120	135	810	515	650	–	–	–	810
45	120	135	810	515	–	–	–	–	850
50	125	–	–	515	–	–	–	–	880
55	120	–	–	515	–	850	–	–	850
60	120	–	–	520	–	850	–	–	885
70	125	–	–	515	–	850	–	–	900
80	120	–	–	520		–	–	875	950
85	–	–	–	–	600	–	–	920	1000
90	–	–	–	–	400	–	–	990	–
95	–	–	–	–	–	–	–	–	–
100	–	–	–	–	–	–	–	–	1290

Table 2 Thermal effects observed on heating samples of the system Ag$_2$Te–Zn

Composition,/ mol% of Zn	Endothermic effects on heating, $T/°C$						
	1	2	3	4	5	6	7
0	150	–	680	–	950	–	950
5	–	145	590	–	855	–	920
10	–	140	550	550	810	–	890
15	–	140	–	–		800	860
20	–	–	–	550	–	800	800
30	–	140	–	550	–	795	835
40	–	140	–	–	–	800	850
45	–	140	–	–	–	805	855
50	–	140	–	–	–	800	860
55	–	140	–	–	–	800	865
60	–	–	–	–	–	–	880
70	–	–	–	–	450	–	750
80	–		–	–	450	–	655
85	–	–	–	–	450	–	625
90	–	–	–	–	450	–	–
95	–	–	–	–	450	–	535
100	–	–	–	–	–	–	420

the sample of X composition (system II) are single phase, while the rest are two-phase systems (Fig. 1).

Most of the two-phase samples of system I were with small grain structure. Hence, the construction of the probability polygons for the empirical distribution of the microhardness (HV) was required. For every composition, even for every phase when this was possible, HV was evaluated (HV is the microhardness average value based on 100 measurements) – Figs 4, 5.

In the concentration ranges from 0 to 9 and from 95 to 100 mol% of ZnTe (system I), and from 0 to 5 mol% Zn (system II), HV varies linearly which is an indication for the presence of solid solutions based on Ag$_2$Te and on ZnTe (Fig. 8). The results from HV measurements show that solid solutions based on Ag$_2$Te (Fig. 9) should be expected in the concentration range from 0 to 5 mol% of Zn.

The results obtained in density (d) measurements are shown in Figs 6 and 7.
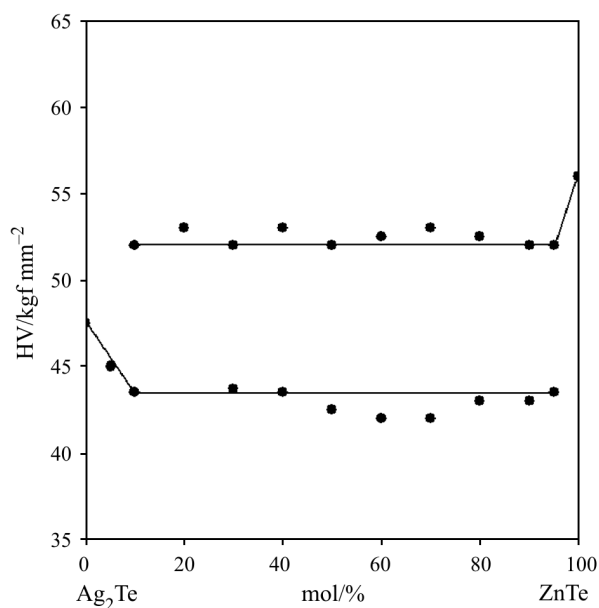
Fig. 4 Samples microhardness for the system Ag$_2$Te–ZnTe
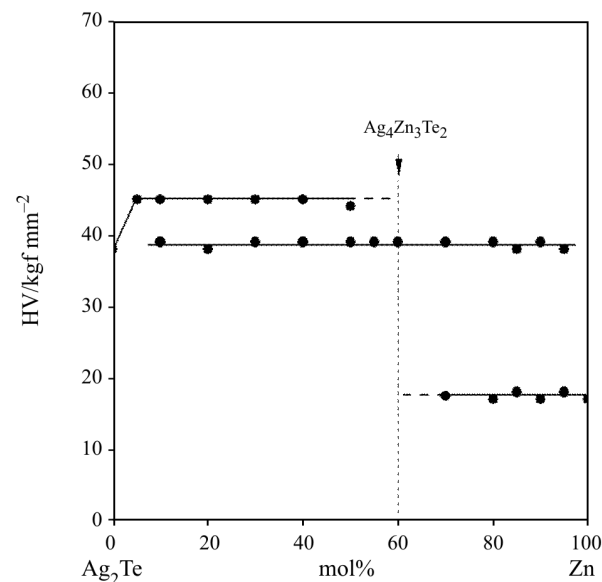
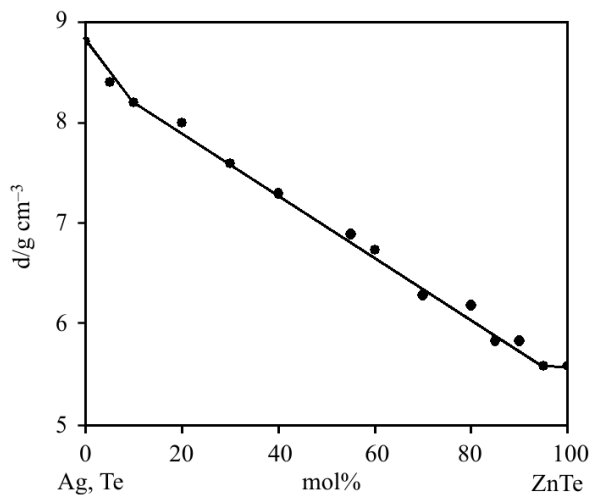**Fig. 5** Samples microhardness for the system Ag$_2$Te–Zn

Fig. 6 Samples density for the system Ag$_2$Te–ZnTe

The regular variation of *d vs. x* in the concentration ranges from 0 to 9 and from 95 to 100 mol% of ZnTe (system I) and from 0 to 5 mol % of Zn (system II) indicates the presence of boundary solutions based on Ag$_2$Te and ZnTe on one hand and on Ag$_2$Te on the other. The characteristic variation of *d vs. x* in the system (Ag$_2$Te)$_{100-x}$Zn$_x$ at *x*=60 is connected with the presence of an intermediate phase Ag$_4$Zn$_3$Te$_2$ (phase X–Fig. 1). The linear variation of *d vs. x* in the concentration ranges from 9 to 95 mol% of ZnTe (system I) as well as from 5 to 60 and from 60 to 100 mol% of Zn (system II) evidences the presence of two-phase areas, Ag$_2$Te+ZnTe as well as Ag$_2$Te+Ag$_4$Zn$_3$Te$_2$ and Ag$_4$Zn$_3$Te$_2$+Zn.

Discussion

On the ground of data obtained by DTA, XRA, MSA and measurements of samples' microhardness and density, the state diagrams of the systems Ag$_2$Te–ZnTe and
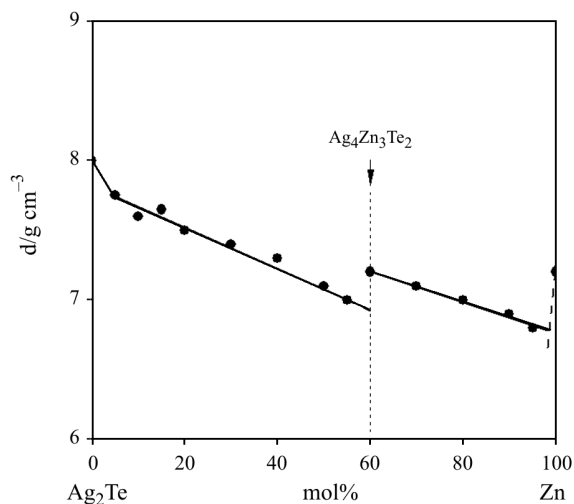

Fig. 7 Samples density for the system Ag$_2$Te–Zn

Ag$_2$Te–Zn were constructed. These are quasi-binary polythermic sections of the ternary system Ag–Zn–Te (Figs 1, 8 and 9).

Ag$_2$Te–ZnTe system

The state diagram of the system Ag$_2$Te–ZnTe (Fig. 8) is characterized by:
- 18 phase regions;
- eutectic reactions at 810±10°C and at 850±10°C (eutectic points at 40 and 55 mol% of ZnTe, respectively);
- three eutectoidal reactions, two of which on Ag$_2$Te side at temperature values 650±10°C and 135±10°C (eutectoidal points at ca 18 and 15 mol% of ZnTe) and one at 120±10°C, resulting in the formation of an intermediate compound Ag$_2$ZnTe$_2$. The latter melts congruently at 880±10°C while at 515±10°C it takes part in a polymorphic transition of the kind α⇔β. Phase transition of the compound is proved by the
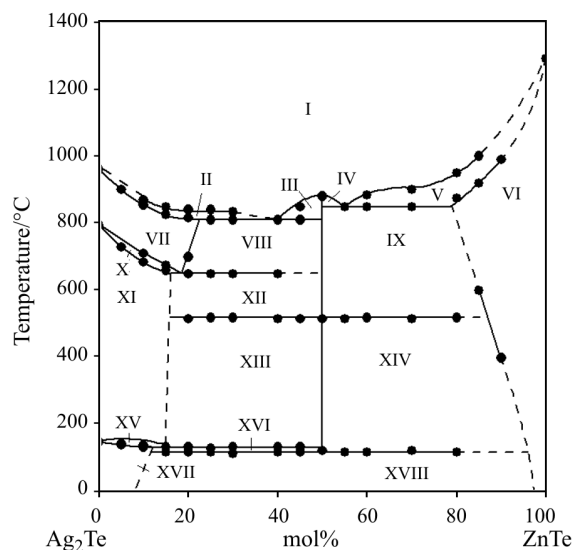
Fig. 8 State diagram of the system Ag$_2$Te–ZnTe (I–L (melt);
II – γ-Ag$_2$Te+L;
III – L+β-Ag$_2$ZnTe$_2$;
IV – β-Ag$_2$ZnTe$_2$+L;
V – L+α′-ZnTe;
VI – α′-ZnTe (solid solution);
VII – γ-Ag$_2$Te (solid solution);
VIII – γ-Ag$_2$Te+β-Ag$_2$ZnTe$_2$;
IX – β-Ag$_2$ZnTe$_2$+α′-ZnTe;
X – β-Ag$_2$Te+γ-Ag$_2$Te;
XI – β-Ag$_2$Te (solid solution);
XII – β-Ag$_2$Te+β-Ag$_2$ZnTe$_2$;
XIII – β-Ag$_2$Te+α-Ag$_2$ZnTe$_2$;
XIV – α-Ag$_2$ZnTe$_2$ +α′-ZnTe;
XV – α-Ag$_2$Te+β-Ag$_2$Te;
XVI – α-Ag$_2$Te+α-Ag$_2$ZnTe$_2$;
XVII – α-Ag$_2$Te (solid solution);
XVIII – α-Ag$_2$Te+α′-ZnTe)

help of DTA and XRD methods described by Abdel-Aziz [18] and Hashimoto *et al.* [19].

When ZnTe content is increased, the temperature of phase transition $\gamma \rightarrow \beta$-Ag_2Te, i.e. from cubic lattice with a bulk centered unit (region VII) to cubic lattice with a wall centered unit (region XI) is decreased. The same is valid for the transition $\beta \rightarrow \alpha$-Ag_2Te, i.e. from cubic lattice with a wall centered unit (region XI) to a monoclinic lattice (region XVII). This difference in the structures determines the existence of two-phase regions X and XV. On temperature increase the solubility of ZnTe in α-, β- and γ-Ag_2Te increases slightly. Region VI corresponds to the solid solutions of ZnTe. The solubility of Ag_2Te in ZnTe increases on temperature increase and it reaches its maximal value at 850°C (~22 mol% of Ag_2Te). The solubility of Ag_2Te in ZnTe decreases on further temperature increase.

At 120°C Ag_2ZnTe_2 gives two solid solutions, which determine the existence of the two-phase region XVIII.

The boundaries of regions XVII and XVIII are verified by DTA, XRA, MSA and microhardness measurements. The boundaries of the rest of the phase areas are verified by DTA. Regions I, VI, VII, XI and XVII are single-phase, while the rest are two-phase.

The state diagram of the system Ag_2Te–ZnTe constructed by us differs from that described in reference [15] mainly in two points:

- the regions of the solid solutions based on α-, β- and γ-Ag_2Te and on ZnTe are essentially larger (in the paper pointed above there is no region of solid solutions based on α-Ag_2Te, see region XVII of the diagram just described);
- an intermediate phase Ag_2ZnTe_2 is formed in the system Ag_2Te–ZnTe which melts congruently at 880±10°C, while in reference [15] there is no data about any intermediate phase. This phase gives α-Ag_2Te and ZnTe at 120±10°C.

Ag₂Te–Zn system

The state diagram of the system Ag_2Te–Zn (Fig. 9) is characterized by:

- 15 phase areas;
- nonvariant eutectic equilibrium at 800±10°C with an eutectic point at 20 mol% of Zn;
- two eutectoidal reactions at 550±10 and 140±10°C with eutectoidal points at ca 13 and ca 8 mol% of Zn and
- one peritectic equilibrium at 450±10°C with a peritectic point at ca 97 mol% of Zn (Fig. 9).

An intermediate phase $Ag_4Zn_3Te_2$ is formed in the system Ag_2Te–Zn. It is found in the temperature range from 20 to 880°C and melts congruently at
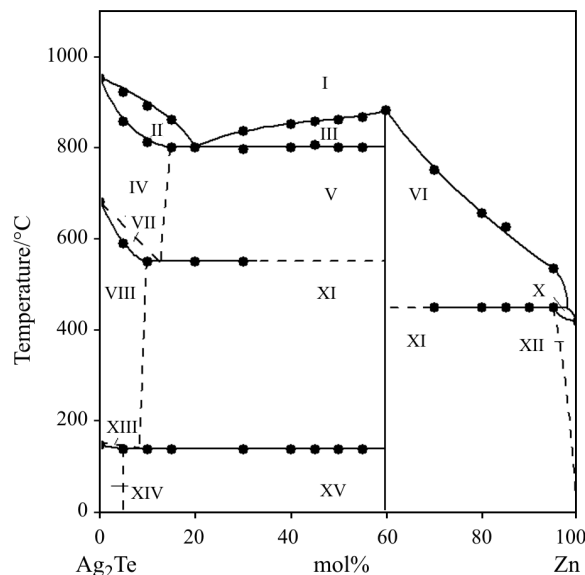

Fig. 9 State diagram of the system Ag_2Te–Zn (I–L (melt);
II – γ-Ag_2Te+L;
III – L+$Ag_4Zn_3Te_2$;
IV – γ-Ag_2Te (solid solution);
V – γ-Ag_2Te+$Ag_4Zn_3Te_2$;
VI – $Ag_4Zn_3Te_2$+L;
VII – β-Ag_2Te+γ-Ag_2Te;
VIII – β-Ag_2Te (solid solution);
IX – β-Ag_2Te+$Ag_4Zn_3Te_2$;
X – α'-Zn+L;
XI – $Ag_4Zn_3Te_2$+α'-Zn;
XII – α'-Zn (solid solution);
XIII – α-Ag_2Te+β-Ag_2Te;
XIV – α-Ag_2Te (solid solution);
XV – α-Ag_2Te+$Ag_4Zn_3Te_2$)

880±10°C. The solubility curves of this phase cross in a singular point at an angle greater than 90°, i.e. it is unstable in the liquid state.

The polymorphism of Ag_2Te determines the existence of three one-phase areas (solid solutions based on α-, β- and γ-Ag_2Te, correspondingly). The solvus-lines of these solid solutions (phase area IV, VIII and XIV) depend on the temperature (the solubility of Zn in α-, β- and γ-Ag_2Te increases on temperature increase). The existence of solid solutions based on α-, β- and γ-Ag_2Te determines the presence of two-phase area VII and XIII. Zn dissolves also Ag_2Te and this solubility increases on temperature increase (region XII). At ambient temperatures Zn does not practically dissolve Ag_2Te.

The boundaries of phase areas XIV, XV and XI are determined by DTA, XPA, MSA as well as HV and *d* measurements, while those of the other areas found by DTA. Phase areas I, IV, VIII, XII and XIV are one-phase, while the rest are two-phase. The solid solutions based on α-Ag_2Te (phase area XIV) present definite interest. They are expected to have semi-con-

ducting properties taking in consideration the alloy-additive functions of Zn in respect to α-Ag$_2$Te.

Conclusions

The state diagrams of the systems Ag$_2$Te–ZnTe(I) and Ag$_2$Te–Zn(II) are constructed on the basis of data obtained by DTA, XRA, MSA and measurements of microhardness and density of samples synthesized. Systems I and II form intermediate compounds Ag$_2$ZnTe$_2$ and Ag$_4$Zn$_3$Te$_2$, respectively, as well as solid solutions based on Ag$_2$Te in areas XVII and XIV, correspondingly. The intermediate compounds melt congruently at 880°C. Ag$_2$ZnTe$_2$ is stable in the temperature range from 120 to 880°C, while Ag$_4$Zn$_3$Te$_2$ is present at temperature values between 20 and 880°C.

Acknowledgements

References

1 G. I. Peetrenco, Z. Anorg. Chem., 48 (1906) 347.
2 H. C. H Carpenter and W. Whitely, Intern. Z. Metallog., 3 (1913) 145.
3 J. Alfred and J. R. Fruch, Amer. Mineralogist, 46 (1961) 654.
4 C. R. Veale, J. Less- Common Metals, 11 (1966) 50.
5 J. Carides and G. Fisher, Solid State Commun., 2 (1964) 217.
6 R. Reynolds, D. G. Stroud and D. A. Stevenson, J. Electrochem. Soc., 114 (1967) 1287.
7 G. Steiniger, R. F. Brebrick and A. J. Strauss, J. Electrochem. Soc., 117 (1970) 1305.
8 H. Hubota, Jap. J. Appl. Phys., 2 (1963) 259.
9 Phizika i himiya soedineniiAIIBVI (pod. Redakcii C.A.Medvedeva), Moscow, Mir (1970) (in Russian).
10 Z. Boncheva-Mladenova and V. S. Vassilev, Himiya i phisikohimiya na poluprovodnikovite materiali, Ministry of Higher Education, Sofia (1991) (in Bulgarian).
11 R. Dalven and R. Gill, Phys. Rev., 143 (1966) 666.
12 R. Dalven, Phys. Rev., 16 (1966) 311.
13 P. P. Petrov, V. S. Vassilev and Z. Boncheva-Mladenova, Phys. Status Solidi, 99 (1987) 237.
14 V. P. Juze, I. M. Tzidilkovskaya and T. S. Bartnizkaya, Zh. Tekh. Fiz., 28 (1958) 1646 (in Russian).
15 L. I. Trischuk, G. S. Olejnik and I. B. Mizeztkaya, Ukr. Khim. Zhurnal, 52 (1986) 799 (in Russian).
16 V. Vassilev, L. Bozhkova, I. Markova, S. Stefanova, Y. Ivanova and V. Vatchkov, J. Mater. Sci., 29 (1994) 1711.
17 V. Danielik, J. Gabčová, J. Therm. Anal. Cal., 76 (2004) 763.
18 M. M. Abdel-Aziz, J. Therm. Anal. Cal., 79 (2005) 709.
19 T. Hashimoto, M. Yoshinaga, Y. Ueda, K. Komazaki, K. Acaoka and S. Wang, J. Therm. Anal. Cal., 69 (2002) 909.